Published in final edited form as:
Pigment Cell Melanoma Res. 2015 March ; 28(2): 184–195. doi:10.1111/pcmr.12330.

Wnt5A promotes an adaptive, senescent-like stress response, while continuing to drive invasion in melanoma cells

Marie R. Webster[1], **Mai Xu**[2], **Kathryn A. Kinzler**[2], **Amanpreet Kaur**[1], **Jessica Appleton**[1], **Michael P. O'Connell**[1], **Katie Marchbank**[1], **Alexander Valiga**[1], **Vanessa M. Dang**[1], **Michela Perego**[1], **Gao Zhang**[1], **Ana Slipicevic**[1], **Frederick Keeney**[1], **Elin Lehrmann**[2], **William Wood III**[2], **Kevin G. Becker**[2], **Andrew V. Kossenkov**[1], **Dennie T. Frederick**[3], **Keith T. Flaherty**[3], **Xiaowei Xu**[4], **Meenhard Herlyn**[1], **Maureen E. Murphy**[1], and **Ashani T. Weeraratna**[1,*]

[1]The Wistar Institute, Philadelphia, PA, 19104

[2]The National Institute on Aging, National Institutes of Health, Baltimore, MD

[3]Massachusetts General Hospital Cancer Center, Boston, Massachusetts

[4]Abramson Cancer Center, University of Pennsylvania, Philadelphia, Pennsylvania

Abstract

We have previously shown that Wnt5A drives invasion in melanoma. We have also shown that Wnt5A promotes resistance to therapy designed to target the $BRAF^{V600E}$ mutation in melanoma. Here, we show that melanomas characterized by high levels of Wnt5A respond to therapeutic stress by increasing p21 and expressing classical markers of senescence, including positivity for senescence-associated β-galactosidase (SA-β-gal), senescence associated heterochromatic foci (SAHF), H3K9Me chromatin marks, and PML bodies. We find that despite this, these cells retain their ability to migrate and invade. Further, despite the expression of classic markers of senescence like SA-β-gal and SAHF, these Wnt5A-high cells are able to colonize the lungs in in vivo tail-vein colony forming assays. This clearly underscores the fact that these markers do not indicate true senescence in these cells, but instead an adaptive stress response that allows the cells to evade therapy and invade. Notably, silencing Wnt5A reduces expression of these markers and decreases invasiveness. The combined data point to Wnt5A as a master regulator of an adaptive stress response in melanoma, which may contribute to therapy resistance.

Introduction

Malignant melanoma is a deadly disease, for which cure rates remain dismal, despite recent advances in therapy. Current standard of care for melanoma patients includes the use of inhibitors to the mutant form of BRAF, in patients carrying the $BRAF^{V600E}$ mutation (Chapman et al., 2011). These drugs have met with initial success, but tumors recur, on average, within 7 months of treatment (Amaria et al., 2012). Canonical Wnt signaling via β-catenin increases sensitivity of melanoma cells to BRAF inhibitors (Biechele et al., 2012). Our laboratory has shown that the non-canonical Wnt ligand, Wnt5A, can promote the

*To Whom Correspondence Should Be Addressed: Ashani T. Weeraratna, Ph.D., The Wistar Institute, Rm 452/454A, 3601 Spruce Street, Philadelphia, PA 19104, Office: 215 495-6937, Fax: 215 495-6938, aweeraratna@wistar.org.

degradation of β-catenin, via SIAH2, an ubiquitin ligase. As such, increases in Wnt5A can promote resistance to the BRAF inhibitor, Vemurafenib (O'Connell et al., 2013), a finding recently supported by others (Anastas et al., 2014). Targeting the Wnt5A pathway, therefore, decreases resistance to Vemurafenib. We have also shown that this switch to a non-canonical Wnt phenotype can be activated by hypoxia, and drives both invasion and therapy resistance (O'Connell et al., 2013). Treating melanoma cells with Vemurafenib induces senescence in a subpopulation of cells, instead of the more desirable apoptosis (Haferkamp et al., 2013). In the current study, we noted that Wnt5A high, but not Wnt5A low cells exposed to Vemurafenib, or other stresses, such as ionizing radiation undergo a senescent-like stress response, but retain invasive capacity. This may be an adaptive response to different forms of stress, which allows the cells to survive. Not being able to drive a subpopulation of cells to a complete, terminal arrest, or apoptosis may lead to a lack of complete and durable response to Vemurafenib.

In melanoma, we have shown that the non-canonical Wnt pathway driven by the ligand Wnt5A confers an invasive phenotype (Weeraratna et al., 2002, Dissanayake et al., 2007, O'Connell et al., 2009a, O'Connell et al., 2009b, O'Connell et al., 2013). Conversely, canonical Wnt signaling plays a role in the early stages of melanoma, bypassing melanocyte senescence and driving proliferation via the master transcriptional regulator MITF. Downstream targets of MITF such as MART-1 (melanoma antigen recognized by T cells-1) are upregulated in early-stage melanoma and are markers of a more proliferative and less invasive state (Dissanayake et al., 2008, Eichhoff et al., 2011) (Dissanayake et al., 2007). Importantly, we have shown that Wnt5A can inhibit the expression of MITF, and subsequently downstream markers such as MART1 (Dissanayake et al., 2008). MITF depletion in melanocytic cells drives a senescent phenotype, (Giuliano et al., 2010) and in an independent study, MITF depletion was shown to drive invasion of melanoma cells (Carreira et al., 2006). This discrepancy suggests that there might be a link between senescence and invasion, and that Wnt5A, although it is a driver of invasion, might also increase markers of senescence in melanoma cells. In support of this premise, Wnt5A was shown to drive senescence in ovarian cancer cells (Bitler et al., 2011).

Senescence is typically defined as a state in which cells terminally arrest. Several forms of senescence have been identified including therapy-induced senescence (Schmitt, 2003), oncogene-induced senescence (Michaloglou et al., 2005), and replicative senescence (Hayflick, 1974); all of these result in growth arrest. Experimentally, senescence is defined by a cohort of markers including senescence-associated β-galactosidase activity (SA-β-gal), senescence-associated heterochromatic foci (SAHF), promyelocytic bodies (PML) and modified chromatin, as defined by the presence of the Histone H3 trimethyl Lys9 (H3K9Me) marks. Very recent data suggest that whereas replicative senescence induced by the breakage of telomeres is believed to be irreversible, other types of senescence may not be. For example, oncogene-induced senescence, by enforced expression of oncogenic HRas or by silencing of the ribonucleotide reductase subunit M2, can be overcome by the replenishment of nucleotides (Aird et al., 2013). However, examples where oncogene or therapy-induced senescence have been shown to be reversible are few, and that senescence can be reversible is not a well-accepted paradigm.

Here, we show that Wnt5A drives a senescent-like response in melanoma cells exposed to diverse forms of stress. Despite the presence of canonical markers of senescence, these cells retain invasive capacity, and are able colonize distant metastatic sites. These data reinforce the premise that the presence of uniform markers of senescence, like SA-β-gal, chromatin marks, PML bodies, SAHF and a growth arrest, do not mean the cell is truly senescent. A better understanding of senescence is needed before we can promote the clinical utility of driving a cell to senescence as a therapeutic endpoint. Importantly, Wnt5A is emerging as a biomarker of not only metastasis in melanoma, but also of therapy resistance.

Results

Wnt5A promotes a senescent-like phenotype in melanoma cells

For this study we selected 6 primary melanoma cell lines derived from patient samples. We previously demonstrated that Wnt5A is abundantly expressed in three of these (FS4, 5, 11), but is very poorly expressed in three others (FS12, 13, 14). We also previously showed that the levels of Wnt5A dictate the invasive potential in these cell lines, with Wnt5A-high lines having high invasive potential, and Wnt5A-low lines with little to no invasive potential (O'Connell et al., 2009a). PKC signaling is increased in the Wnt5A-high lines as would be expected, as this kinase is downstream of Wnt5A (Supplementary Figure 1A). Additionally, MITF and MART1, a downstream target of MITF, are decreased in Wnt5A-high cells, consistent with previous findings (Dissanayake et al., 2008, Eichhoff et al., 2011) (Supplementary Figure 1A, B). Since MITF depletion has been associated with senescence (Giuliano et al., 2010), and Wnt5A decreases MITF and MART1 (Dissanayake et al., 2008, Eichhoff et al., 2011), we investigated whether markers of senescence could be increased by Wnt5A in melanoma cells.

We first sought to determine whether Wnt5A-high cells demonstrated increased senescence in the presence of therapeutic stress. MTS assays indicated that Wnt5A-high cells are more resistant to PLX4720 than Wnt5A-low cells (Supplemental Figure 1C). FS13 cells, which do not have the BRAF mutation, do not respond to PLX4720, as expected (Supplementary Figure 1D), so for additional cell line we used the Wnt5A low, PLX4720 sensitive WM35 and 451Lu (see Supplementary Figure 1C, O'Connell et al., 2013). Wnt5A-high cells were treated with 5μM PLX4720 for 5 days, and show a significant increase in SA-β-galactosidase staining (Figure 1A), as compared to Wnt5A low cells. Additional cell lines are shown in Supplementary Figure 1E. Next, we tested ionizing radiation as a different form of stress. Cells were irradiated with 10 Gy γ-radiation and examined 5 days later for the presence of senescence associated SA-β–galactosidase positive cells. In response to irradiation, Wnt5A-high cells exhibited significantly greater levels of β–galactosidase positivity than did Wnt5A-low cells (Figure 1B). Quantitation of stain for β–galactosidase assays are shown in Supplementary Figure 1F (PLX4720) and Supplementary Figure 1G (irradiation). These changes are not attributable to differences in the rates of proliferation of the cells, as we see no consistent differences in proliferation (Supplementary Figure 1H).

The presence of SA-β–galactosidase positive cells is not considered to be sufficient evidence for senescence. Therefore, we analyzed these cells for other markers of senescence, including the presence of senescence-associated heterochromatin foci (SAHF), H3K9Me

chromatin marks and PML bodies. Wnt5A high cells demonstrate increased H3K9Me and SAHF upon exposure to either irradiation or PLX4720, a BRAF inhibitor, as compared to Wnt5A low cells (Supplementary Figure 2A–C). An analysis of PML bodies revealed that there was a greater increase in PML bodies in Wnt5A-high cells following PLX4720 (Figure 1C,D) and irradiation (Figure 1E,F). Further, at 5 days, FACs analysis shows that an increased number of cells treated with either PLX4720 or irradiation remain arrested (Supplementary Figure 2D,E).

We next sought to perform an unbiased analysis of the result of stress in Wnt5A high and Wnt5A low cells. Toward this goal we performed microarray analysis of Wnt5A high vs. Wnt5A low cells, in the presence and absence of radiation. In irradiated cells, we found that 173 genes were significantly upregulated by day 5 post-irradiation in Wnt5A high cells, compared to Wnt5A-low cells. Of these, 5 out of the top 6 most changed genes were markers of the senescence-associated secretory phenotype, including IL1A, CSF2, SERPINB2, CXCL2, MMP3 and CCL20 (Supplementary Figure 2F). Similarly, untreated Wnt5A high cells exhibited increases in the cytokines IL6, IL8 and GM-CSF, compared to Wnt5A low cells; these cytokines are known to be hallmarks of the senescence-associated secretory phenotype (SASP) previously observed in senescent fibroblasts (Coppe et al., 2010). We confirmed these results by real time PCR (Supplementary Figure 2G).

To determine whether Wnt5A could drive increases in SA-β–galactosidase activity in melanoma cells, we analyzed the effects of Wnt5A on SA-β–galactosidase activity. In general we found that Wnt5A high cells express more basal SA-β–galactosidase activity than Wnt5A low cells (Figure 1G,H, compare untreated panels). Further, we found that treatment of Wnt5A low FS13 cells with recombinant Wnt5A (rWnt5A) led to increased SA-β–galactosidase activity (Figure 1G). Conversely, knockdown of Wnt5A in Wnt5A high cells decreases baseline SA-β–galactosidase activity (Figure 1H). Knockdown of Wnt5A also decreased the SA-β–galactosidase positive cells in Wnt5A high cells after irradiation, and treatment of Wnt5A low cells with rWnt5A, increased SA-β–galactosidase after irradiation (Figure 1G,H). This is reflected also in the growth arrest patterns observed, where Wnt5A treatment of Wnt5A low cells increases growth arrest (Supplementary Figure 2H) and knockdown of Wnt5A in Wnt5A high cells decreases IR-induced growth arrest (Supplementary Figure 2I). Taken together, these data confirm that Wnt5A can drive a senescent-like phenotype in melanoma cells, both at a baseline level, and in response to therapeutic stress.

Wnt5A regulates p21 expression in melanoma

In an effort to further examine the response of Wnt5A high and Wnt5A low melanoma cells to Wnt5A signaling and radiation, we next examined the expression of the senescence associated markers p16 and p21, by Western blot analysis. Interestingly, in invasive Wnt5A high cells, p21 is highly expressed, and p16 is not (Figure 2A). In contrast, in Wnt5A low cells, p16 is highly expressed, and p21 is undetectable (Figure 2A). The loss of p21 protein in the Wnt5A low cells is not due to mutation, as we were able to confirm that CDKN1A is wild type in FS13 and 14; similarly p16 loss is not attributed to deletion or mutation of the CDKN2A gene in the Wnt5A high cell lines (Supplementary Table 1). To determine if the

Wnt5A pathway could itself affect levels of p21, we treated Wnt5A low cells with recombinant Wnt5A (rWnt5A), and analyzed the level of p21. Treatment of Wnt5A-low melanoma cells with rWnt5A resulted in an increase in p21, but inconsistent effects on p16 (Figure 2B). Phospho-CAMKII is shown as a positive control for signaling downstream of rWnt5A. Conversely, knocking down Wnt5A in Wnt5A high cells resulted in a decrease in p21 (Figure 2C). P16 was undetectable in these cells.

We then tested the ability of irradiation and targeted therapy to increase p21 in Wnt5A high cells. Irradiation increased p21 in Wnt5A high, but not low cells (Figure 2D). Notably, similar to the response to radiation, increases in expression of Wnt5A and p21 are observed after 5 days of treatment with 1 μM PLX4720 in Wnt5A high cells (Figure 2E), but not in Wnt5A low cells (Figure 2F). BRAFi-resistant subclones of WM983B cells also demonstrate increased Wnt5A and p21, confirming the importance of these molecules in the generation of resistance (Figure 2G). We have previously shown that Wnt5A promotes resistance to BRAF inhibition (O'Connell et al., 2013), a finding recently supported by others (Anastas et al., 2014). Our previous studies indicated that samples from patients with a poor clinical response to Vemurafenib (less than 30% response by RECIST), or samples from tumors from patients who relapsed after an initial response expressed high levels of Wnt5A (O'Connell et al., 2013). To determine whether p21 was highly expressed in relapsed samples or samples with a low response rate, we stained 9 samples from patients who exhibited a RECIST response of less than 30%, or which were samples of recurrent, relapsed tumors. Of these 7 exhibited high levels of p21 staining (Supplementary Table 2). Of four samples with a strong response to Vemurafenib (greater than 30% response), 2 were negative for p21, 1 had moderate positivity, and one had weak positivity for p21. Even in this small sample set, when the Wilcoxon rank-sum (Mann-Whitney) test was used for two group comparisons, the p21 score was significantly different between groups ($p=0.046$). Moreover, the percent of response has significantly negative correlation with p21 score (Spearman's $r=-0.77$, $p=0.002$) Shown as a comparison are samples with >30% response rate, which show little p21 expression, as compared to ones with a <30% response rate (Figure 2H).

Wnt5A high cells continue to invade following therapeutic stress

The effect of Wnt5A in promoting a senescent-like phenotype following therapeutic stress was surprising, given the data from our lab and others which demonstrate that high levels of Wnt5A are typically associated with more aggressive, resistant melanomas. These previous findings suggest that these cells might retain the ability to migrate and invade, despite the presence of markers of senescence. Indeed, our microarray analysis suggests that a migratory phenotype might persist in Wnt5A high cells, even 5 days after irradiation, despite the fact that the cells show markers of senescence (Supplementary Figure 3). To determine whether Wnt5A high cells retain their ability to migrate post-irradiation, cells were irradiated, and seeded on Matrigel®-coated transwell chambers at 1, 3 and 5 days after irradiation. Remarkably, we found that Wnt5A high cells retain their ability to invade, despite the presence of senescence markers (Figure 3A). Notably, knockdown of Wnt5A using siRNA resulted in an inhibition of this invasive potential (Figure 3B). Similarly,

treatment of Wnt5A low cells with rWnt5A increased the ability of the cells to migrate, and this incease in migration was not affected by irradiation (Figure 3C).

Next, we asked whether the invading cells were growth arrested or proliferating. To address this, we irradiated Wnt5A high cells, subjected them to a Boyden chamber invasion assay, and then assessed the cell cycle profile (propidium iodide staining) and BrdU incorporation of both invaded (bottom chamber) and non-invaded (top chamber) cells. As expected, non-irradiated cells showed a normal, asynchronous cell cycle profile, whether they invaded or not (Figure 3D, compare the red and blue bars). Interestingly, cell cycle analysis and BrdU staining of the irradiated cells indicates that a significant portion of both invaded and non-invaded cells show evidence of a G2/M cell cycle arrest (Figure 3E). To determine whether cells that invade retain their senescence markers once they have migrated, we irradiated cells, allowed them five days to upregulate markers of senescence, and then subjected them to a Boyden chamber invasion assay. Cells which invaded through the membrane were assessed for SA-β-galactosidase staining. Migrated Wnt5A high cells express β–galactosidase positivity (Figure 3F). Of the very few Wnt5A low cells that invade, none are β–galactosidase positive (Figure 3F). We also performed a wound-healing assay on cells five days following irradiation, on which we then performed SA-β-galactosidase staining. Wnt5A high cells continue to stain positive for SA-β-galactosidase, even while migrating into a scratch wound, whereas Wnt5A low cells do not (Figure 3G).

To address the possibility that vemurafenib-treated cells might also be senescent-like but capable of invasion, we treated BRAF-mutant Wnt5A high and Wnt5A low cells with the BRAF inhibitor PLX4720 and analyzed their therapeutic and metastatic responses. As the case with ionizing radiation, many of the “senescent-like” Wnt5A high cells, but not the Wnt5A low cells, retain significant invasive ability after 5 days of PLX4720 (Figure 3H), and this invasiveness increases with increased doses of PLX4720. To ensure that it was the senescent-like cells that were migrating, we treated Wnt5A high and low cells for 5 days with 5μM of PLX4720. Then, cells were treated with C_{12}FDG, a fluorescent marker for SA-β-galactosidase activity. Time lapse imaging confirmed that Wnt5A high, but not low, cells treated with PLX4720 increase their levels of SA-β-galactosidase as determined by C_{12}FDG fluorescence, and that these “senescent” cells continue to migrate into the scratch wound (Figure 3I, Supplementary Movies). These combined data indicate that Wnt5A high cells retain the ability to migrate and invade, even in the presence of markers of senescence.

Wnt5A high cells that appear senescent are capable of forming colonies in vivo

If these senescent-like cells are invasive, but incapable of growing out at distant sites, then they do not represent a particularly threatening subpopulation of cells. Therefore, we next sought to test the hypothesis that the apparent growth arrest of irradiated, invasive cells might be transient and/or reversible. We also sought to test the hypothesis that, following resumption of proliferation, these cells might retain their senescent markers, such as SA-β-galactosidase staining. To determine whether these senescent-like cells could form new tumors in vivo, we irradiated Wnt5A high cells and after 5 days, injected them into mice via the tail vein. Notably, 8 out of 10 mice injected with irradiated cells developed significant lung tumors, indicating that these irradiated, growth-arrested cells were likely capable of re-

initiating proliferation (Figure 4A). Knocking down Wnt5A in the Wnt5A high cells resulted in an ablation of metastasis formation as we have previously shown (Dissanayake et al., 2008), with only one animal showing encapsulated tumor cells in a blood vessel (Supplementary Figure 4A–C). In the tumors derived from irradiated cells, a significant percentage of the cells retained SA-β–galactosidase positivity (Figure 4B), whereas the tumors from non-irradiated cells did not. Finally, staining of the lung colonies also demonstrated increased SAHF in lung colonies generated from irradiated cells (Figure 4C). To more formally test the hypothesis that the growth-arrested, Wnt5A-high cells could resume proliferation, we irradiated Wnt5A high cells, and five days later examined the cell cycle profile. Five days following irradiation, there was still an increase in the percentage of irradiated cells in G2/M compared to untreated cells (Figure 4D). We then irradiated Wnt5A high cells, and five days later sorted the cells in G0/G1 and G2/M (growth arrested), and plated both populations into colony forming assays. Notably, both the G0/G1 and the G2/M sorted cells were capable of forming colonies in vitro (Figure 4E), suggesting that the G2/M arrest was transient. We also analyzed the expression of Wnt5A and p21 in the G2/M and G0/1 sorted cells by Western. Cells in G2/M exhibit increased Wnt5A, and increased p21 (Figure 4F). These data are consistent with the premise that the growth arrest induced by radiation was transient, but the markers of senescence were stable; in support of this, we noted several cells from the lung metastases that were positive for both Ki-67 and SA-β-gal (Figure 4G). These combined data indicate that the Wnt5A pathway controls a stress response that confers upon cells the markers of senescence, but with the retained ability to invade and proliferate at distant metastatic sites.

Discussion

Driving cells to senescence via strategies that include the reactivation of p53, inhibition of CDKs or inhibition of oncogenes such as Myc, has garnered much interest as an approach for cancer therapy (Schmitt, 2003, Tai and Chung, 2007, Lleonart et al., 2009, Acosta and Gil, 2012). However, our understanding of the implications of senescence in tumor growth and metastasis remain limited. In the current study, we show that highly invasive melanoma cells express Wnt5A and p21, and undergo a growth arrest when exposed to diverse forms of stress such as ionizing irradiation, or targeted therapy (PLX4720). This growth arrest is somewhat deceptive however, as it bears the hallmarks of senescence, yet the cells remain highly invasive, and retain the ability to form new colonies (metastases). Our data are consistent with data showing that depletion of MITF, which we have shown is also suppressed by Wnt5A (Dissanayake et al., 2008), drives both senescence and invasion. We purport that this Wnt5A-driven, senescent-like response may be an adaptive stress mechanism in aggressive melanoma cells, allowing tumors to evade therapy, by undergoing a growth arrest that prevents them from incorporating further damage. We show here two divergent forms of stress, BRAF inhibition and ionizing radiation, and the similarities between the adaptive stress response in both cases indicates that this may be a general response to multiple forms of stress.

Senescent-like responses in response to Vemurafenib have been previously observed. It has been suggested that the observation that a subpopulation of melanoma cells will senesce upon treatment with Vemurafenib may underlie the re-emergence of tumors at the same sites

that initially responded to therapy (Haferkamp et al., 2013). Other work has also shown that where TGFβ induces a senescent-like, slow growing phenotype in melanoma, exposure of melanoma cells to TGFβ in the presence of Vemurafenib can subsequently promote proliferation, suggesting that the observed senescence is not terminal (Sun et al., 2014). Finally, data from Haq et al suggest that melanoma cells reprogram themselves metabolically to circumvent Vemurafenib induced senescence (Haq et al., 2014). All of these data are consistent with our observation that a subpopulation of Wnt5A high cells undergo a senescent-like adaptive stress response, but retain invasive and proliferative capability.

The role of senescence in tumor progression is truly complex. Senescence of stromal cells may either suppress or drive tumor invasion depending upon the cellular context (Coppe et al., 2010). Interestingly, our Wnt5A-high senescent-like tumor cells express factors very similar to those secreted by senescent fibroblasts, termed the “senescence associated secretory phenotype” or SASP. Work from the Campisi laboratory has shown that this SASP can drive tumor invasion (Coppe et al., 2010). Our data presented in this study suggest that melanoma cells can also produce a SASP, and these SASP-producing cells are invasive, implying that they may be driving their own invasion. What is intriguing is the fact that these invaded cells, can go on to form colonies in vitro and in vivo, showing that this phenotype was never truly senescence, despite the fact that the cells are positive for a wide range of senescence markers (β-gal, H3K9Me, SAHF and PML bodies). The negative implications of this are clear- there is much interest in the field of therapy-induced senescence, which suggests that if we cannot kill a tumor cell, the next best thing is to stop it growing. Our data suggest that in fact, some tumor cells can mimic a senescent-like phenotype, but retain highly aggressive characteristics, a phenomenon we term “pseudosenescence”. This lends caution on two different fronts- one, we clearly do not have effective markers for “true” senescence, and two, relying on these markers to declare a therapy effective may be very misleading. In fact, in a subpopulation of cells, i.e., highly invasive cells that express high Wnt5A, and p21, this senescence-like phenotype and growth arrest may even promote metastasis, as suggested by the increased invasion and metastasis of treated as compared to untreated highly invasive cells that we observed in our in vivo colony forming assays. The role of Wnt5A in this process is also of interest, because Wnt5A plays very different roles in different cancers. In breast cancer and ovarian cancer it may act as a tumor suppressor, and at least in ovarian cancer this may be due to the ability of Wnt5A to promote a senescent-like phenotype (Bitler et al., 2011). Why this senescent-like response correlates with increased invasion in melanoma, but not in ovarian cancer will require further investigation. As with many other processes in tumorigenesis the outcome may be truly tissue and context dependent (Bissell, 2009).

The phenomenon of a senescent-like, yet highly invasive phenotype has implications beyond tumor biology in the interpretation of basic experimental cell biology findings as well as in aging related studies. Therefore, the next step is to uncover the mechanisms leading to true, irreversible senescence. Data from Schmitt et al indicate that p16 expression can drive a true, irreversible senescence, with positive outcome in mouse models (Schmitt et al., 2002). However, p21 may be involved in reversible senescence phenotypes (Macip et al., 2002), in agreement with the data presented here. As shown here, we see differences in the cohorts of

cell cycle markers (p21, p16) in the senescent-like phenotype. In addition, growth factor signaling through receptors such as FGFR3 may also contribute to a reversible form of cellular senescence (Krejci et al., 2010). Together, these data indicate that SA-β–galactosidase is an unreliable marker of true senescence, and we may need to rely more heavily on genetic markers such as p16 and p21, as well as measure other factors, including the rate of invasion and Wnt5A expression, in order to truly assess senescence in the laboratory or in the clinic. Indeed, it has been shown that melanomas can be forced to undergo terminal senescence when transfected with p16 (Haferkamp et al., 2008), and it has been shown that this is the “normal” mode of senescence in melanocytes (Gray-Schopfer et al., 2006). P16 is often deleted, or otherwise silenced in melanoma, which implies that a p16 driven senescence is less beneficial to the tumor cell, while, perhaps, a p21 driven senescence might improve its chances of survival, especially after exposure to stress.

Together, our data suggest that treatments that would eradicate one subpopulation of tumor cells, may actually drive the aggressive, resistant nature of a second subpopulation of tumor cells. A better understanding of senescence and its effects on the tumor cell, as well as improvements in the current arsenal of tools available to study senescence, are required before we can contemplate the use of senescence as an endpoint for tumor therapy. Schmitt et al suggest that we can harness the senescent phenotype, and its associated enzymes to target and kill slow growing tumor cells (Dorr et al., 2013). Indeed, this may be a viable strategy for cancer therapy even in cases such as those we present here, where senescence-associated markers are associated with invasion.

Materials and Methods

Cell Culture

FS cell lines were maintained in RPMI 1640 supplemented with 10% fetal bovine serum (Invitrogen, Carlsbad, CA) and with 100 U/ml penicillin and streptomycin and 4 mM L-glutamine. WM35, 1205Lu and 451Lu were maintained in MCDB153/Leibovitz’s L-15 (80/20%) supplemented with 2% FCS and 2 mM $CaCl_2$. All cells were cultured at 37°C in 5% CO_2. Cell stocks were fingerprinted using AmpFLSTR® Identifiler® PCR Amplification Kit from Life Technologies TM at The Wistar Institute Genomics Facility. Although it is desirable to compare the profile to the tissue or patient of origin, our cell lines were established before acquisition of normal control DNA was routinely performed. However, each STR profile is compared to our internal database of over 200 melanoma cell lines as well as control lines such as HeLa and 293T. STR profiles are available upon request. Cell culture supernatants were mycoplasma tested using a Lonza MycoAlert assay at the University of Pennsylvania Cell Center Services.

Wnt5A and Irradiation treatment

Cells were treated with 100 ng/ml of recombinant Wnt5A (R&D Systems, Minneapolis, MN) for 16 hours unless otherwise stated. For cell cycle analysis, cells were treated with rWnt5A for 16 hours, and 1 hour before irradiation additional rWnt5A was added to the media. Cells were irradiated with either 10 Gy (Nordian Gammacell 40 extractor, 1.22 Gy/

min) for initial experiments or 2.8 Gy (J.L. Sheppard Irradiator, 2.83 Gy/min) for all remaining experiments.

siRNA Transfection

Cells were transfected with high-performance (HP)-validated negative control (CTRL), Wnt5A siRNA and ROR2 siRNA (Qiagen, Venlo, Netherlands) using Lipofectamine (Invitrogen) for 48–72 hours as described previously (Dissanayake et al., 2007). *WNT5A* sequences have been previously described and tested by microarray analysis for off-target effects (Dissanayake et al., 2007).

shRNA Infection

Wnt5A shRNA was obtained from the TRC shRNA library available through the Molecular Screening Facility at The Wistar Institute. Clones used were:

TRCN0000062717 – CGTGGACCAGTTTGTGTGCAA

TRCN0000062716 – CACATGCAGTACATCGGAGAA

Lentiviral production was carried out as described in the protocol developed by the TRC library (Broad Institute). Briefly, 293T cells were co-transfected with Wnt5a shRNA vector and lentiviral packaging plasmids (pCMV-dR8.74psPAX2, pMD2.G). The supernatant containing virus was harvested at 36 and 60 hours, combined and filtered through a 0.45μm filter. For transduction, FS4 cells were layered overnight with lentivirus containing 8 μg/ml polybrene. The cells were allowed to recover for 24 hours and then selected using 1μg/ml puromycin.

Invasion Assay

Invasion assays were performed using transwell migration chambers (Corning Life Sciences, Lowell, MA). The 8 μm filters were coated with 150 μL of 80 μg/ml Matrigel (Becton Dickinson, Franklin Lakes, NJ). Cells were seeded onto the filters in serum free media at 2×10^5 cells/well. To measure the effect of irradiation on invasion, the FS cell lines were first irradiated (10 G), and then seeded onto the filters. To measure the effect of drug treatment on invasion, the FS cell lines were treated with drug for 5 days, and then seeded onto the filters at 7×10^4 cells. Media containing 20% FCS was placed in the lower well to act as a chemoattractant. Cells were allowed to invade and adhere to the lower chamber, stained using crystal violet, and counted.

Western Blotting

Total protein lysate (50–65 μg) was run on a 4–12% NuPAGE Bis Tris gel (Invitrogen). Proteins were then transferred and blocked as previously described (O'Connell et al., 2009b). Primary antibodies were used at the following concentrations: Biotinylated Wnt5a (500 ng/ml, R&D systems), MART-1 (400 ng/ml, Neo Markers), p16 (1:500, Sigma, St. Louis, MO), p21 (1:1000, Cell Signaling, Danvers, MA), HSP90 (1:4000, Cell Signaling), β-tubulin (0.5 μg/ml) (Cell Signaling) All primary antibodies were diluted in 5% milk/TBST and incubated over night at 4°C. The membranes were washed in TBST and probed with the corresponding HRP-conjugated secondary antibody (0.2–0.02 μg/ml of anti-mouse,

streptavidin, or anti-rabbit). Proteins were visualized using, ECL prime (Amersham, Uppsala, Sweden), or Luminata Crescendo (Millipore, Billerica, MA).

Cell Cycle Analysis

Cell cycle distribution was measured using flow cytometry. Cells were seeded and treated with irradiation (10 or 2.8 G), rWnt5A or siRNA as stated above. At 8 and 16 hours post-irradiation, the media was collected, and the remaining cells were washed with PBS. The cells were then collected using a cell dissociation enzyme (TrypLE, invitrogen). Samples were pelleted by centrifugation (1,500 rpm for 3 min) and washed with 1% FBS/PBS. Next, cells were centrifuged (1,500 rpm for 3 min), resuspended in 1 ml PBS, and fixed with 9 ml cold 70% ethanol and incubated at 4° C for 30 min. Cells were washed with 1% FBS/PBS and resuspended in 2:1 1%FBS in PBS/phosphate citric acid buffer (pH 7.8). Cells were incubated at room temperature for 5 min, centrifuged (1,500 rpm for 3 min), resuspended in 300 μL PBS/FBS/PI/RNase (10 μg/ml propidium iodide and 3 KU RNaseA), and incubated at 37° C for 30 min. The DNA content of the cells was analyzed by flow cytometry (BD LSRII 14 color).

Illumina oligonucleotide microarray

Transcriptional profiling was determined using Illumina Sentrix BeadChips. Total RNA was used to generate biotin-labeled cRNA using the Illumina TotalPrep RNA Amplification Kit. In short, 0.5ug of total RNA was first converted into single-stranded cDNA with reverse transcriptase using an oligo-dT primer containing the T7 RNA polymerase promoter site and then copied to produce double-stranded cDNA molecules. The double stranded cDNA was cleaned and concentrated with the supplied columns and used in an overnight in-vitro transcription reaction where single-stranded RNA (cRNA) was generated incorporating biotin-16-UTP. A total of 0.75ug of biotin-labeled cRNA was hybridized at 58°C for 16 hours to Illumina's Sentrix Human HT-12 v3 Expression BeadChips (Illumina, San Diego, CA). Each BeadChip has around 48,000 transcripts with approximately 15-fold redundancy. The arrays were washed, blocked and the labeled cRNA was detected by staining with streptavidin-Cy3. Hybridized arrays were scanned using an Illumina BeadStation 500X Genetic Analysis Systems scanner and the image data extracted using the Illumina GenomeStudio software, version 1.1.1). Data are available in the GEO database, under accession #GSE50004.

Microarray analysis

Preprocessing. Microarray data was log2 transformed, quantile normalised and probes that showed low expression levels (detection p-value>0.05) across all 16 samples (2 replicates × 2 cell lines H/L × 4 time points d0, 1h, 24h, d5) were removed from the analysis.
Differential expression. Significance Analysis of Microarrays (SAM (Zhang, 2007)) was used to find differentially expressed genes between any two conditions using "Two class unpaired" option and False Discovery Rate (FDR) was estimated using the Storey et. al. (Storey and Tibshirani, 2003) procedure. Only probes that changed at least 1.5 fold (FC) with FDR<15% were called significant unless stated otherwise.

Cell Sorting

Cells were irradiated with 2.8 Gy of γ-radiation and 16 hours post-irradiation, media, washes and cells were collected. Cells were counted and resuspended at a concentration of 1×10^6 cells/500 μL 1% FBS/RPMI. Cells were stained with Hoechst 3342 dye (2ug/ml) for 45 min at 37° C. Cells in G0/1 and G2/M of the cell cycle were then sorted on a BD ARIAII.

Colony Forming Assay

Cells were seeded at 3×10^3 or 5×10^3 cells in 5 ml media per 60 mm dish. Dishes were incubated at 37° C 5% CO_2 until colonies formed. Once colonies were visible, the cells were washed with 3 ml PBS and stained with crystal violet (0.5% in 75% methanol) for 5 min at room temperature. Cells were then rinsed in cold water and dried at room temperature.

Tail Vein Metastases Assay

All animal experiments were approved by the Institutional Animal Care and Use Committee (IACUC) (IACUC #112503Y_0) and were performed in an Association for the Assessment and Accreditation of Laboratory Animal Care (AAALAC) accredited facility. FS4 irradiated (2.8 G) and non-irradiated cells (1×10^6 cells/100 μl PBS) were injected into the tail vein of female athymic nude mice (Charles River Laboratories, Wilmington, MA). After 4 weeks, the mice were euthanized, the lungs were harvested, half of the tissue was embedded in paraffin and half in optimal cutting temperature compound (O.C.T, Sakura, Japan City) and flash frozen for sectioning.

Immunofluorescence

Cells were seeded into two well slide chambers (Nunc, Rochester, NY) at 2×10^4 cells/well and incubated overnight. Next, cells were either irradiated (2.8 G) or treated with rWnt5A (100ng/ml for 16 h), followed by (+/−) irradiation. Cells were then fixed at 1, 4, 8, and 16 hours post-irradiation and blocked as previously described (O'Connell et al., 2009b). Primary antibodies were diluted in blocking buffer and incubated over night at 4° C. Slides were washed in PBS and incubated with appropriate secondary diluted in blocking buffer (1:2000, Alexa fluor-488 or Alexa Fluor-568, (Invitrogen) for one hour at room temperature. Slides were then washed in PBS and mounted in Prolong Gold anti-fade reagent containing DAPI (Invitrogen). Images were captured on a LSM 710 confocal microscope (Zeiss) or a TE2000 inverted microscope (Nikon).

Immunohistochemistry (IHC)

Patient samples were collected under IRB exemption approval for protocol #EX21205258-1. Samples were stained for p21 expression using p21 (1:100, Cell Signaling, Danvers, MA). Paraffin embedded sections were rehydrated through a xylene and alcohol series, rinsed in H2O and washed in PBS. Antigen retrieval was performed using target retrieval buffer (Vector Labs, Burlingame, CA) and steamed for 25 minutes. Samples were then blocked in a peroxidase blocking buffer (Thermo Scientific) for 15 minutes, followed by an Ultra-V block (Thermo Scientific) for 5 minutes, and incubated in p21 primary antibody diluted in blocking buffer at 4°C overnight in a humidified chamber. Following washing in PBS, samples were incubated in a Streptavidin-HRP solution at room temperature for 20 minutes.

Samples were then washed in PBS, and incubated in 3-Amino-9-Ethyl-l-Carboazole (AEC) chromogen for 15 minutes. Finally, samples were washed in H2O, incubated in Mayers hematoxylin for 1 min, rinsed in cold H2O, and mounted in Aquamount. P21 expression was scored by a board certified dermatopathologist (Xiaowei Xu).

β–galactosidase staining

FS cell lines were plated in two well slide chambers. Following irradiation or treatment with rWnt5A cells were washed with PBS and fixed using a fixative solution (Biovision, San Francisco, CA). The cells were incubated at room temperature for 5 min and washed 3 × 5 min in PBS. The slides were then incubated in staining solution at 37° C over-night. The staining solution contained 150 mM NaCl (Sigma, St. Louis, MO), 2 mM $MgCl_2$ (Sigma), 5 mM $K_3Fe(CN)_6$ (Millipore), 5 mM $K_4Fe(CN)_6$ (Millipore), 40 mM Na_2PO_4 (Sigma) pH 5.5, 20 mg/ml X-gal (Applichem, Darmstadt, Germany) in ddH_2O.

β–galactosidase staining of mouse lung tissue

Lung tissue was embedded in O.C.T and flash frozen immediately after it was harvested. The tissues were then sectioned and stained with β–galactosidase as described above.

3D Spheroid Assay

Tissue culture treated 96 well plates were coated with 50 μl 1% Difco Agar Noble (Becton Dickinson). WM3918, M93, and FS11 cells were seeded at 5×10^3 cells/well and allowed to form spheroids over 72 hours. Spheroids were harvested and placed in a collagen plug containing EMEM, FBS, L-Glutamine, sodium bicarbonate, and collagen type I (Organogenesis). The collagen plug was allowed to set and 1 ml RPMI with 10% FBS or DMEM with 5% FBS was added to the top of the plug. For rWnt5A treatment, 100 ng/ml of rWnt5A was added to the collagen plug as well as the media added to the top. The media was spiked with 100 ng/ml of rWnt5A every 24 h. Irradiated spheroids were treated with 2.8 G of γ-radiation.

BrdU Incorporation assay

Cell proliferation was detected by a bromodeoxyuridine(BrdU) flow kit (BD Pharmingen, San Jose, CA) according to the user manual. Briefly, cells were labeled with 10μM BrdU for one hour before they were fixed, permeabilized and subjected to DNaseI treatment. Cells were then stained with FITC-conjugated anti-BrdU antibody and 7-AAD, followed by flow cytometry analysis using a FACSCalibur apparatus(BD Pharmingen, San Jose, CA).

Real Time PCR

RNA was extracted using Trizol (Invitrogen) and a RNeasy Mini kit (Qiagen) as previously described (O'Connell et al., 2009a). Gene expression was quantified using SYBR green method of qPCR and mRNA levels were compared to standard curves. Primers were designed to cross intron-exon junctions where possible. qPCR was performed on an ABI StepOnePlus sequence detection system using fast conditions and samples were normalized against the 18S gene, using Universal 18S primers (Ambion, Austin, TX). Expression was

calculated using the standard curve method according to the manufacturer's protocol (Perkin Elmer, Waltham, MA).

Cell Proliferation Assay (MTS)

Cell Proliferation was determined using CellTiter 96 Aqueous One Solution Cell Proliferation Assay according to manufacturers protocol. Cells were seeded at 6.5 × 103 cells per well in flat bottom 96-well plates and allowed to adhere overnight. The next day, cells were treated with 0 to 10 mM PLX4720/1% DMSO for 24 hours. Following treatments, cells were incubated with MTS dye (20 μl/well) for 2 h. Absorbance was determined at 490nm using an EL800 microplate reader (BioTek, Winooski, VT). The percent cell proliferation was calculated by converting the experimental absorbance to percentage of control and plotted vs drug concentration. The values were then analyzed using a nonlinear dose-response analysis in GraphPad Prism.

Time Lapse Imaging

Cells were treated with 1μM PLX4720 for 96h, and then treated with C12FDG. A scratch would was inflicted on the monolayer. Six well plates were imaged using a Nikon Te300 inverted microscope equipped with a motorized XY stage and environmental chamber (Temperature and CO2 control surrounding entire microscope). Image Pro 7.0 was used for image acquisition but also controls the motorized stage, filter wheels, shutters, and lamp settings. Using the automated stage macro, twelve areas were selected, 2 fields per well, locations in any X, Y, or Z direction saved. The experiment was set up for 24 hours, acquiring images at the saved x,y,z positions every 10 minutes, using an Imaging Retiga EX, high sensitivity monochrome camera, with a 1360 × 1036 pixel resolution.

Supplementary Material

Refer to Web version on PubMed Central for supplementary material.

Acknowledgments

We thank Drs. Chi V. Dang (Abramson Cancer Center, University of Pennsylvania, Philadelphia, PA), Kenneth Kinzler (Sidney Kimmel Cancer Center, Johns Hopkins University), Mina Bissell (Lawrence Berkeley Laboratories, CA), Daniel Peeper, (Netherlands Cancer Institute), Andrew Aplin (Thomas Jefferson University, PA) and Rugang Zhang, Dmitry Gabrilovich and Dario Altieri (The Wistar Institute) for critical reading of the manuscript. We thank Dr. Jessie Villanueva (The Wistar Institute) for the use of the WM983B resistant cells. We thank Dr. Kate Nathanson for assistance with sequencing of the cell lines. We also thank Dr. Qin Liu for assistance with statistics. This work was supported in part by funds from the Intramural Program of the National Institute on Aging, Baltimore, MD, P01 CA 114046-06 (MH, ATW, GZ, KM, MEM) and RO1 CA174746-01 (ATW).

References

ACOSTA JC, GIL J. Senescence: a new weapon for cancer therapy. Trends Cell Biol. 2012; 22:211–9. [PubMed: 22245068]

AIRD KM, ZHANG G, LI H, TU Z, BITLER BG, GARIPOV A, WU H, WEI Z, WAGNER SN, HERLYN M, ZHANG R. Suppression of nucleotide metabolism underlies the establishment and maintenance of oncogene-induced senescence. Cell Rep. 2013; 3:1252–65. [PubMed: 23562156]

AMARIA RN, LEWIS KD, JIMENO A. Vemurafenib: the road to personalized medicine in melanoma. Drugs Today (Barc). 2012; 48:109–18. [PubMed: 22384451]

ANASTAS JN, KULIKAUSKAS RM, TAMIR T, RIZOS H, LONG GV, VON EUW EM, YANG PT, CHEN HW, HAYDU L, TORONI RA, LUCERO OM, CHIEN AJ, MOON RT. WNT5A enhances resistance of melanoma cells to targeted BRAF inhibitors. J Clin Invest. 2014; 124:2877–90. [PubMed: 24865425]

BIECHELE TL, KULIKAUSKAS RM, TORONI RA, LUCERO OM, SWIFT RD, JAMES RG, ROBIN NC, DAWSON DW, MOON RT, CHIEN AJ. Wnt/beta-catenin signaling and AXIN1 regulate apoptosis triggered by inhibition of the mutant kinase BRAFV600E in human melanoma. Sci Signal. 2012; 5:ra3. [PubMed: 22234612]

BISSELL M. Mina Bissell: Context is everything. [An interview by Ben Short]. J Cell Biol. 2009; 185:374–5. [PubMed: 19414604]

BITLER BG, NICODEMUS JP, LI H, CAI Q, WU H, HUA X, LI T, BIRRER MJ, GODWIN AK, CAIRNS P, ZHANG R. Wnt5a suppresses epithelial ovarian cancer by promoting cellular senescence. Cancer Res. 2011; 71:6184–94. [PubMed: 21816908]

CARREIRA S, GOODALL J, DENAT L, RODRIGUEZ M, NUCIFORO P, HOEK KS, TESTORI A, LARUE L, GODING CR. Mitf regulation of Dia1 controls melanoma proliferation and invasiveness. Genes Dev. 2006; 20:3426–39. [PubMed: 17182868]

CHAPMAN PB, HAUSCHILD A, ROBERT C, HAANEN JB, ASCIERTO P, LARKIN J, DUMMER R, GARBE C, TESTORI A, MAIO M, HOGG D, LORIGAN P, LEBBE C, JOUARY T, SCHADENDORF D, RIBAS A, O'DAY SJ, SOSMAN JA, KIRKWOOD JM, EGGERMONT AM, DRENO B, NOLOP K, LI J, NELSON B, HOU J, LEE RJ, FLAHERTY KT, MCARTHUR GA. Improved survival with vemurafenib in melanoma with BRAF V600E mutation. N Engl J Med. 2011; 364:2507–16. [PubMed: 21639808]

COPPE JP, DESPREZ PY, KRTOLICA A, CAMPISI J. The senescence-associated secretory phenotype: the dark side of tumor suppression. Annu Rev Pathol. 2010; 5:99–118. [PubMed: 20078217]

DISSANAYAKE SK, OLKHANUD PB, O'CONNELL MP, CARTER A, FRENCH AD, CAMILLI TC, EMECHE CD, HEWITT KJ, ROSENTHAL DT, LEOTLELA PD, WADE MS, YANG SW, BRANT L, NICKOLOFF BJ, MESSINA JL, BIRAGYN A, HOEK KS, TAUB DD, LONGO DL, SONDAK VK, HEWITT SM, WEERARATNA AT. Wnt5A regulates expression of tumor-associated antigens in melanoma via changes in signal transducers and activators of transcription 3 phosphorylation. Cancer Res. 2008; 68:10205–14. [PubMed: 19074888]

DISSANAYAKE SK, WADE M, JOHNSON CE, O'CONNELL MP, LEOTLELA PD, FRENCH AD, SHAH KV, HEWITT KJ, ROSENTHAL DT, INDIG FE, JIANG Y, NICKOLOFF BJ, TAUB DD, TRENT JM, MOON RT, BITTNER M, WEERARATNA AT. The Wnt5A/protein kinase C pathway mediates motility in melanoma cells via the inhibition of metastasis suppressors and initiation of an epithelial to mesenchymal transition. J Biol Chem. 2007; 282:17259–71. [PubMed: 17426020]

DORR JR, YU Y, MILANOVIC M, BEUSTER G, ZASADA C, DABRITZ JH, LISEC J, LENZE D, GERHARDT A, SCHLEICHER K, KRATZAT S, PURFURST B, WALENTA S, MUELLER-KLIESER W, GRALER M, HUMMEL M, KELLER U, BUCK AK, DORKEN B, WILLMITZER L, REIMANN M, KEMPA S, LEE S, SCHMITT CA. Synthetic lethal metabolic targeting of cellular senescence in cancer therapy. Nature. 2013; 501:421–5. [PubMed: 23945590]

EICHHOFF OM, WEERARATNA A, ZIPSER MC, DENAT L, WIDMER DS, XU M, KRIEGL L, KIRCHNER T, LARUE L, DUMMER R, HOEK KS. Differential LEF1 and TCF4 expression is involved in melanoma cell phenotype switching. Pigment Cell Melanoma Res. 2011; 24:631–42. [PubMed: 21599871]

GIULIANO S, CHELI Y, OHANNA M, BONET C, BEURET L, BILLE K, LOUBAT A, HOFMAN V, HOFMAN P, PONZIO G, BAHADORAN P, BALLOTTI R, BERTOLOTTO C. Microphthalmia-associated transcription factor controls the DNA damage response and a lineage-specific senescence program in melanomas. Cancer Res. 2010; 70:3813–22. [PubMed: 20388797]

GRAY-SCHOPFER VC, CHEONG SC, CHONG H, CHOW J, MOSS T, ABDEL-MALEK ZA, MARAIS R, WYNFORD-THOMAS D, BENNETT DC. Cellular senescence in naevi and immortalisation in melanoma: a role for p16? Br J Cancer. 2006; 95:496–505. [PubMed: 16880792]

HAFERKAMP S, BECKER TM, SCURR LL, KEFFORD RF, RIZOS H. p16INK4a-induced senescence is disabled by melanoma-associated mutations. Aging Cell. 2008; 7:733–45. [PubMed: 18843795]

HAFERKAMP S, BORST A, ADAM C, BECKER TM, MOTSCHENBACHER S, WINDHOVEL S, HUFNAGEL AL, HOUBEN R, MEIERJOHANN S. Vemurafenib induces senescence features in melanoma cells. J Invest Dermatol. 2013; 133:1601–9. [PubMed: 23321925]

HAQ R, FISHER DE, WIDLUND HR. Molecular Pathways: BRAF Induces Bioenergetic Adaptation by Attenuating Oxidative Phosphorylation. Clin Cancer Res. 2014; 20:2257–63. [PubMed: 24610826]

HAYFLICK L. The strategy of senescence. Gerontologist. 1974; 14:37–45. [PubMed: 4470459]

KREJCI P, PROCHAZKOVA J, SMUTNY J, CHLEBOVA K, LIN P, AKLIAN A, BRYJA V, KOZUBIK A, WILCOX WR. FGFR3 signaling induces a reversible senescence phenotype in chondrocytes similar to oncogene-induced premature senescence. Bone. 2010; 47:102–10. [PubMed: 20362703]

LLEONART ME, ARTERO-CASTRO A, KONDOH H. Senescence induction; a possible cancer therapy. Mol Cancer. 2009; 8:3. [PubMed: 19133111]

MACIP S, IGARASHI M, FANG L, CHEN A, PAN ZQ, LEE SW, AARONSON SA. Inhibition of p21-mediated ROS accumulation can rescue p21-induced senescence. EMBO J. 2002; 21:2180–8. [PubMed: 11980715]

MICHALOGLOU C, VREDEVELD LC, SOENGAS MS, DENOYELLE C, KUILMAN T, VAN DER HORST CM, MAJOOR DM, SHAY JW, MOOI WJ, PEEPER DS. BRAFE600-associated senescence-like cell cycle arrest of human naevi. Nature. 2005; 436:720–4. [PubMed: 16079850]

O'CONNELL MP, FIORI JL, BAUGHER KM, INDIG FE, FRENCH AD, CAMILLI TC, FRANK BP, EARLEY R, HOEK KS, HASSKAMP JH, ELIAS EG, TAUB DD, BERNIER M, WEERARATNA AT. Wnt5A activates the calpain-mediated cleavage of filamin A. J Invest Dermatol. 2009a; 129:1782–9. [PubMed: 19177143]

O'CONNELL MP, FIORI JL, XU M, CARTER AD, FRANK BP, CAMILLI TC, FRENCH AD, DISSANAYAKE SK, INDIG FE, BERNIER M, TAUB DD, HEWITT SM, WEERARATNA AT. The Orphan Tyrosine Kinase Receptor, ROR2, Mediates Wnt5A Signaling in Metastatic Melanoma. Oncogene. 2009b

O'CONNELL MP, MARCHBANK K, WEBSTER MR, VALIGA AA, KAUR A, VULTUR A, LI L, HERLYN M, VILLANUEVA J, LIU Q, YIN X, WIDURA S, NELSON J, RUIZ N, CAMILLI TC, INDIG FE, FLAHERTY KT, WARGO JA, FREDERICK DT, COOPER ZA, NAIR S, AMARAVADI RK, SCHUCHTER LM, KARAKOUSIS GC, XU W, XU X, WEERARATNA AT. Hypoxia Induces Phenotypic Plasticity and Therapy Resistance in Melanoma via the Tyrosine Kinase Receptors ROR1 and ROR2. Cancer Discov. 2013; 3:1378–93. [PubMed: 24104062]

PARK JW, JANG MA, LEE YH, PASSANITI A, KWON TK. p53-independent elevation of p21 expression by PMA results from PKC-mediated mRNA stabilization. Biochem Biophys Res Commun. 2001; 280:244–8. [PubMed: 11162506]

SCHMITT CA. Senescence, apoptosis and therapy--cutting the lifelines of cancer. Nat Rev Cancer. 2003; 3:286–95. [PubMed: 12671667]

SCHMITT CA, FRIDMAN JS, YANG M, LEE S, BARANOV E, HOFFMAN RM, LOWE SW. A senescence program controlled by p53 and p16INK4a contributes to the outcome of cancer therapy. Cell. 2002; 109:335–46. [PubMed: 12015983]

STOREY JD, TIBSHIRANI R. Statistical significance for genomewide studies. Proc Natl Acad Sci U S A. 2003; 100:9440–5. [PubMed: 12883005]

SUN C, WANG L, HUANG S, HEYNEN GJ, PRAHALLAD A, ROBERT C, HAANEN J, BLANK C, WESSELING J, WILLEMS SM, ZECCHIN D, HOBOR S, BAJPE PK, LIEFTINK C, MATEUS C, VAGNER S, GRERNRUM W, HOFLAND I, SCHLICKER A, WESSELS LF, BEIJERSBERGEN RL, BARDELLI A, DI NICOLANTONIO F, EGGERMONT AM, BERNARDS R. Reversible and adaptive resistance to BRAF(V600E) inhibition in melanoma. Nature. 2014; 508:118–22. [PubMed: 24670642]

TAI AW, CHUNG RT. p53 restoration leads to tumor senescence and regression: implications for cancer therapy. Gastroenterology. 2007; 133:722–3. [PubMed: 17681193]

WEERARATNA AT, JIANG Y, HOSTETTER G, ROSENBLATT K, DURAY P, BITTNER M, TRENT JM. Wnt5a signaling directly affects cell motility and invasion of metastatic melanoma. Cancer Cell. 2002; 1:279–88. [PubMed: 12086864]

ZHANG S. A comprehensive evaluation of SAM, the SAM R-package and a simple modification to improve its performance. BMC Bioinformatics. 2007; 8:230. [PubMed: 17603887]

Significance

The need for improving the efficacy and duration of therapies designed to treat cancer is critical. There is much interest in the field of therapy-induced senescence, which suggests that if we cannot kill a tumor cell, the next best thing is to stop it growing. Our data suggest that some tumor cells can mimic a senescent-like phenotype as a generalized response to tumor therapy, but retain highly aggressive characteristics. Our data have implications not only for cancer biology, but also for aging, revealing the fact that the experimental markers of senescence upon which we currently rely, do not always indicate a truly senescent state. Ultimately, driving cells to apoptosis remains the key path to success in the treatment of cancer.

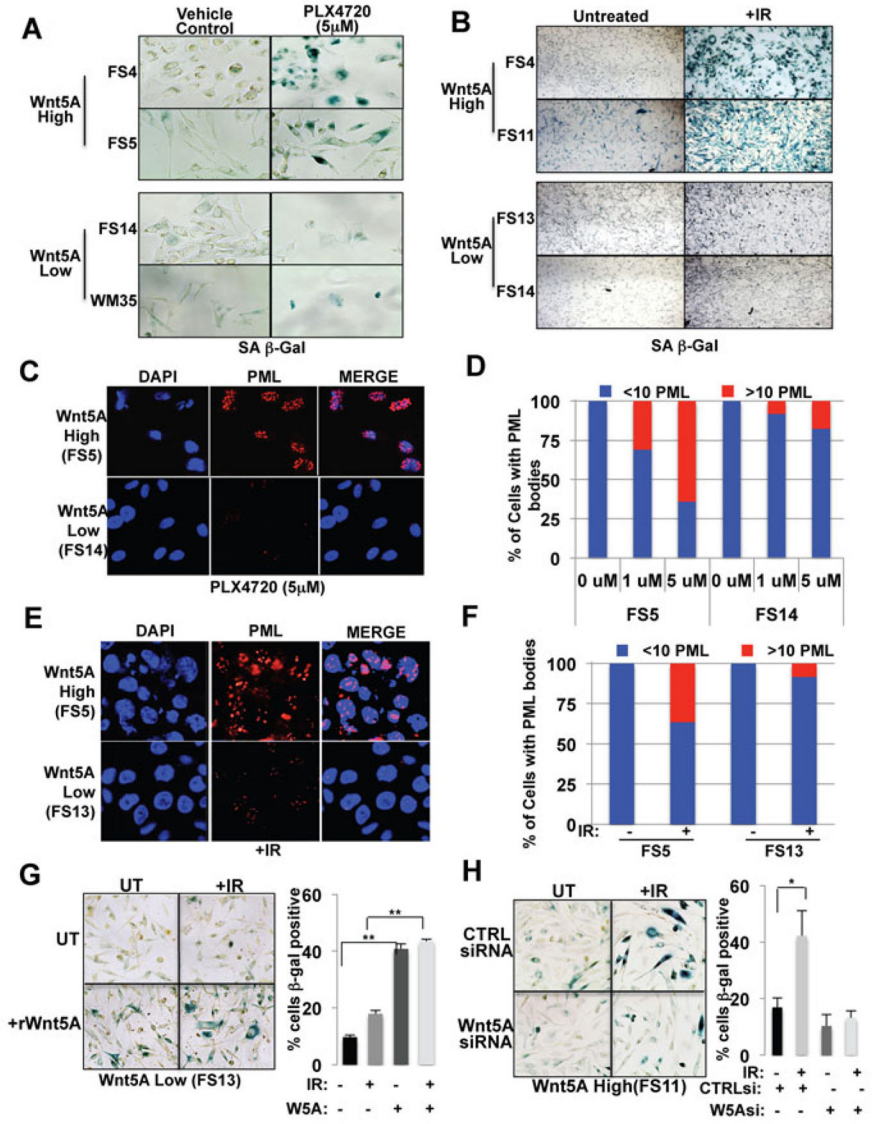

Figure 1. Wnt5A increases markers of senescence in melanoma cells

(A) Wnt5A-high cells were positive for SA-β–galactosidase whereas Wnt5A-low cells were largely dead at 5 days post- treatment with PLX4720. (B) SA-β-galactosidase staining in Wnt5A high and Wnt5A low cells after irradiation. (C) Immunofluorescent analysis of PML bodies following 5 days of treatment with PLX4720. (D) Quantification of changes in PML bodies in response to 5 days of PLX4720 treatment. (E) Immunofluorescent analysis of PML 5 days post irradiation. (F) Quantification of changes in PML bodies in Wnt5A-high and –low cells 5 days following irradiation. (G) Treating Wnt5A-low cells with rWnt5A results in an increase in basal levels of SA-β–galactosidase, as well as an increase after irradiation. (H) Wnt5A high cells express basal levels of SA-β–galactosidase and knockdown of Wnt5A results in a decrease in the number of SA-β–galactosidase positive cells before and after irradiation.

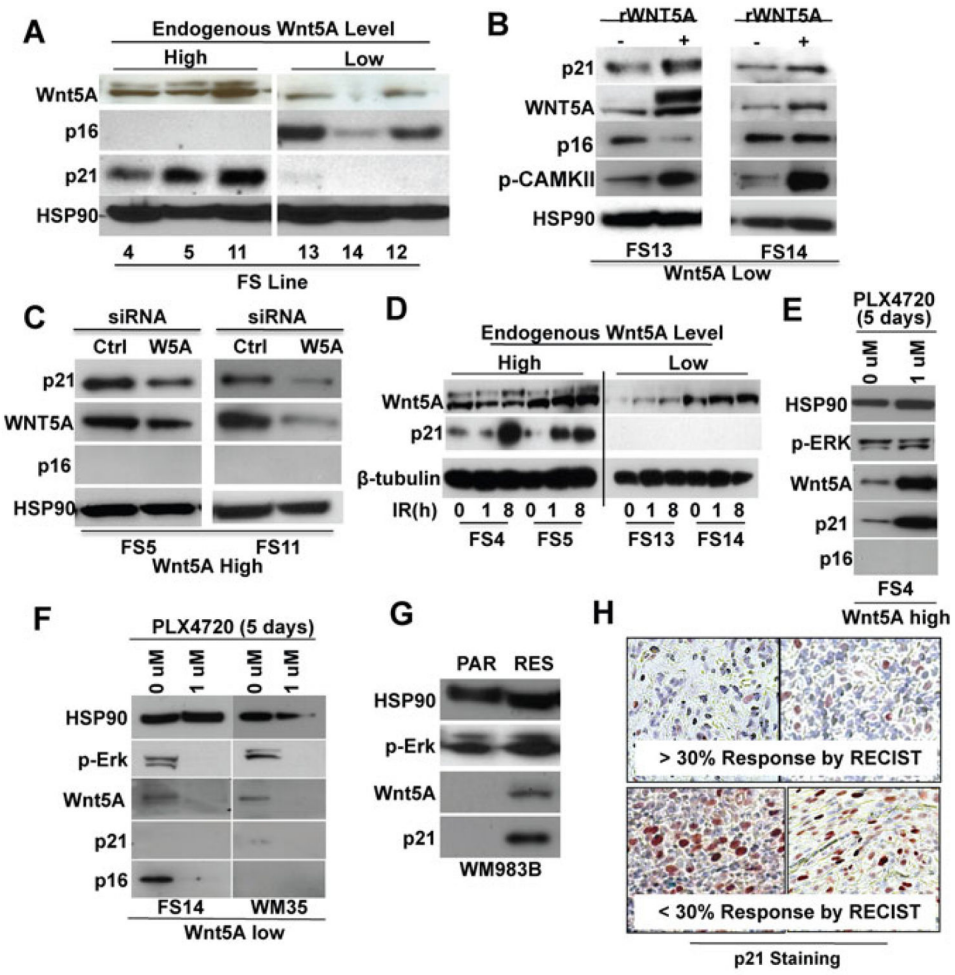

Figure 2. Wnt5A regulates p21 expression in melanoma

(A) Western analysis of cell cycle regulators, p16 and p21 in Wnt5A-high and Wnt5A-low cells. (B) Treatment of Wnt5A-low cells with rWnt5A increases p21 expression. Phospho-CAMKII is shown as a marker of Wnt5A signaling. (C) Knockdown of Wnt5A in Wnt5A-high cells decreases p21 expression by Western analysis. (D) p21 expression increases in Wnt5A high cells following irradiation. (E,F) p21 expression remains high in (E) Wnt5A-high melanoma cells following 5 days of treatment with PLX4720, but not in (F) Wnt5A-low melanoma cells. (G) WM983B parental (PAR) and PLX4720- resistant (RES) WM983B cells were analyzed for Wnt5A and p21. (H) Patient samples with > 30% and <30% response by RECIST were stained for p21 expression by IHC.

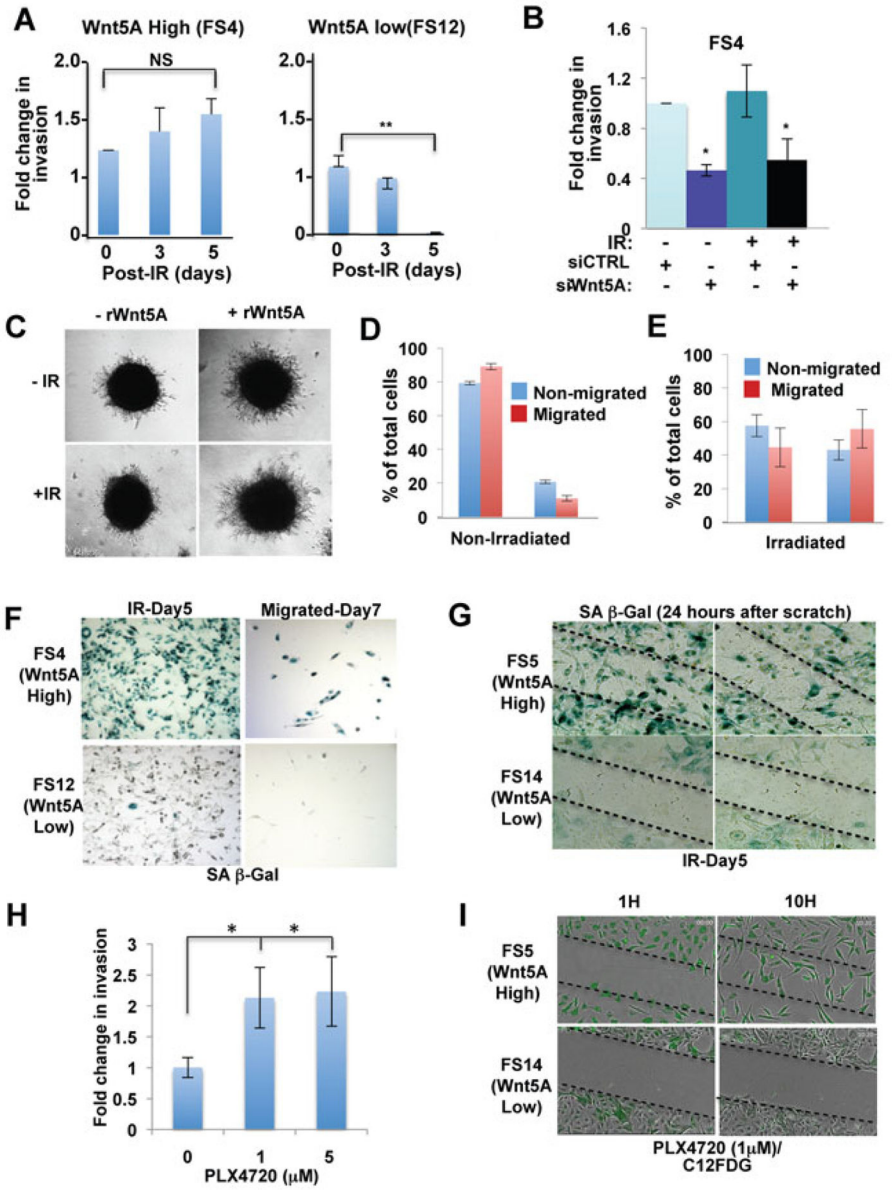

Figure 3. Senescent-like cells retain invasive properties

(A) Wnt5A-high cells continue to invade 1, 3, and 5 days post-irradiation, measured using an invasion assay. The fold change in invasion at each time point was calculated compared to invasion on day 0. (B) Knockdown of Wnt5A in highly invasive (FS4) cells results in the inability of the cells to invade pre- and post- irradiation, measured using an invasion assay. (C) Wnt5A-low cells treated with rWnt5A in a 3D spheroid assay showed increased invasion in the absence of irradation, and retain this ability to invade post irradiation. (D,E) BrdU incorporation assays of Wnt5A-high (FS) cells indicate that there is little difference in the percentage of cells in G2/M between invaded and non-invaded cells either before (D) or after (E) irradiation. (F) Five days following irradiation, cells were plated into an invasion assay for 48 h. Invaded (bottom chamber) Wnt5A-high cells stain positive for SA-β–galactosidase. (G) Wound healing assay demonstrates that Wnt5A high cells invading into

the scratch wound stain positive for SA-β–galactosidase. Wnt5A low cells neither invade, nor stain positive for SA-β–galactosidase. (H) Wnt5A high cells are invasive following treatment with PLX4720 for five days. (I) Time-lapse imaging of PLX4720 treated Wnt5A high and low cells labeled with the fluorescent marker of SA-β–galactosidase, C_{12}FDG, and subjected to a wound-healing assay (see also supplemental movies).

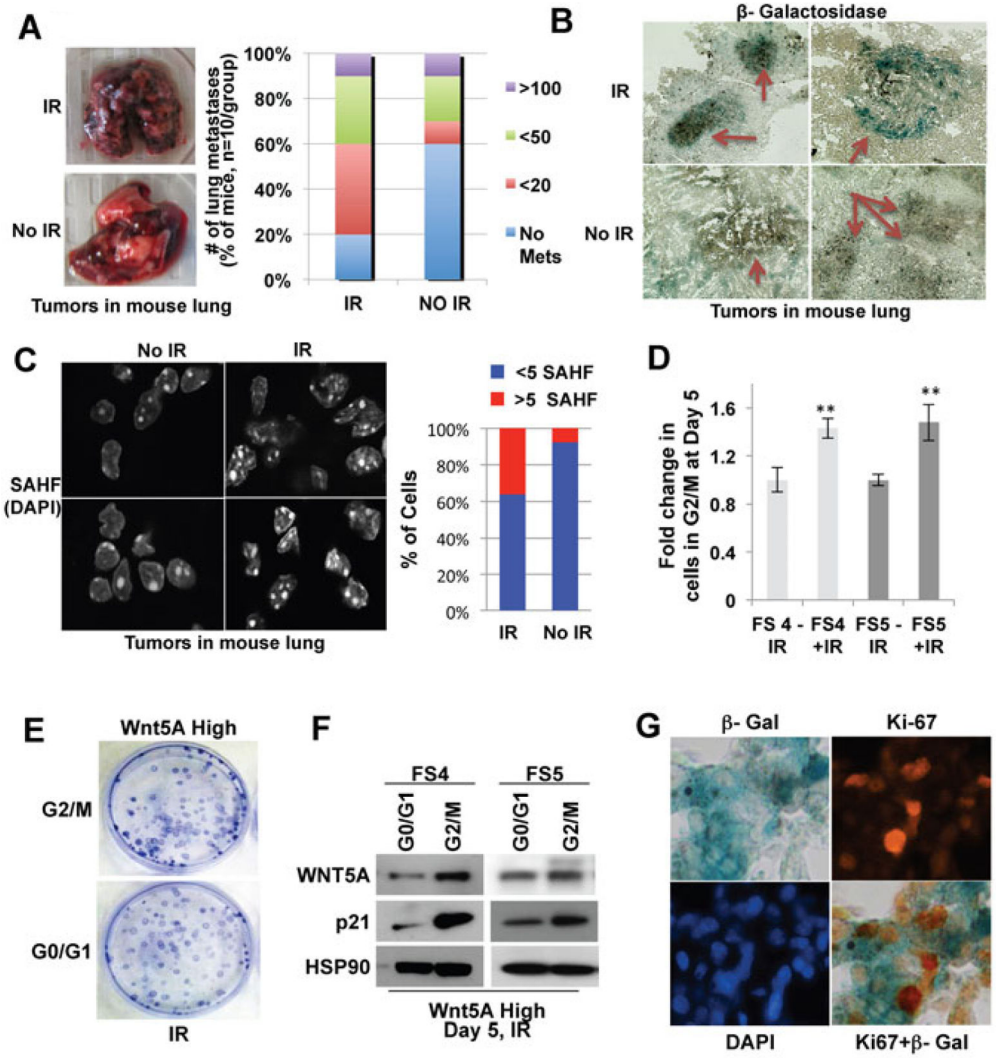

Figure 4. Wnt5A high cells retain clonogenic properties in vitro and in vivo following stress

(A) FS4 cells were injected via the tail vein into mice to perform in vivo colony forming assays. Shown are two representative lungs from mice four weeks after injection with irradiated or non-irradiated invasive cells, and graphical representation of the severity of metastases in both groups (n=10 mice/group). (B) Frozen sections of mouse lung were stained for SA-β–galactosidase. Nests of tumor cells are indicated by arrows. (C) SAHF were identified and quantitated in sections from mouse lungs. (D) Five days following irradiation, there is still a significant increase in the percentage of irradiated cells in G2/M compared to untreated cells. (E) Highly invasive cells were irradiated, sorted into G0/1 and G2/M, and were seeded into colony forming assays. (F) Colonies from G2/M sorted cells retain higher expression of p21 and Wnt5A. (G) Overlay of SA-β–galactosidase and Ki67 in mouse lungs from mice injected with irradiated cells.